

Integration of Extended MHD and Kinetic Effects in Global Magnetosphere Models

Amitava Bhattacharjee

Center for Heliospheric Physics

Department of Astrophysical Sciences
and Princeton Plasma Physics
Laboratory

Princeton University



Our Team

- Amitava Bhattacharjee, PI, [Ammar Hakim](#), and [Liang Wang \(UNH\)](#), *Princeton University/PPPL*
- Kai Germaschewski, Li-Jen Chen, [Li-Wei Lin](#), and Joachim Raeder, *UNH*
- William Daughton, [Adam Steiner](#), LANL
- Homa Karimabadi, [Ari Le](#), and Y. Omelchenko *UCSD*
- John Dorelli, Alex Gloer, [Ilja Honkonen](#), [Chris Bard](#), *NASA-GSFC*

This is a highly leveraged program, involving faculty, research scientists, postdocs, and graduate student(s).

LWS-NASA/NSF Partnership for Collaborative Space Weather Modeling

- NSF: Princeton, UCSD
- NASA: UNH, LANL, NASA-GSFC
- Of the eight awardees, this effort is primarily one dedicated to global magnetosphere modeling.

Team Coordination:

- Monthly telecon and meet once in 6 months. One meeting typically at Fall AGU and/or GEM. Annual meeting at Princeton University.
- Set and monitor milestones.

Primary Objective/Team Coordination

- Our central objective:

Deliver a global magnetosphere code to CCMC which integrates extended MHD and kinetic effects, with verification and validation with observations.

Today's presentation:

- *Overview and progress on integration of kinetic effects* : A. Bhattacharjee
- *Next generation OpenGGCM*: K. Germaschewski
- *Importance of electron and ion kinetic effects in global simulations*: H. Karimabadi

Desiderata of Capabilities in Global Magnetosphere Code

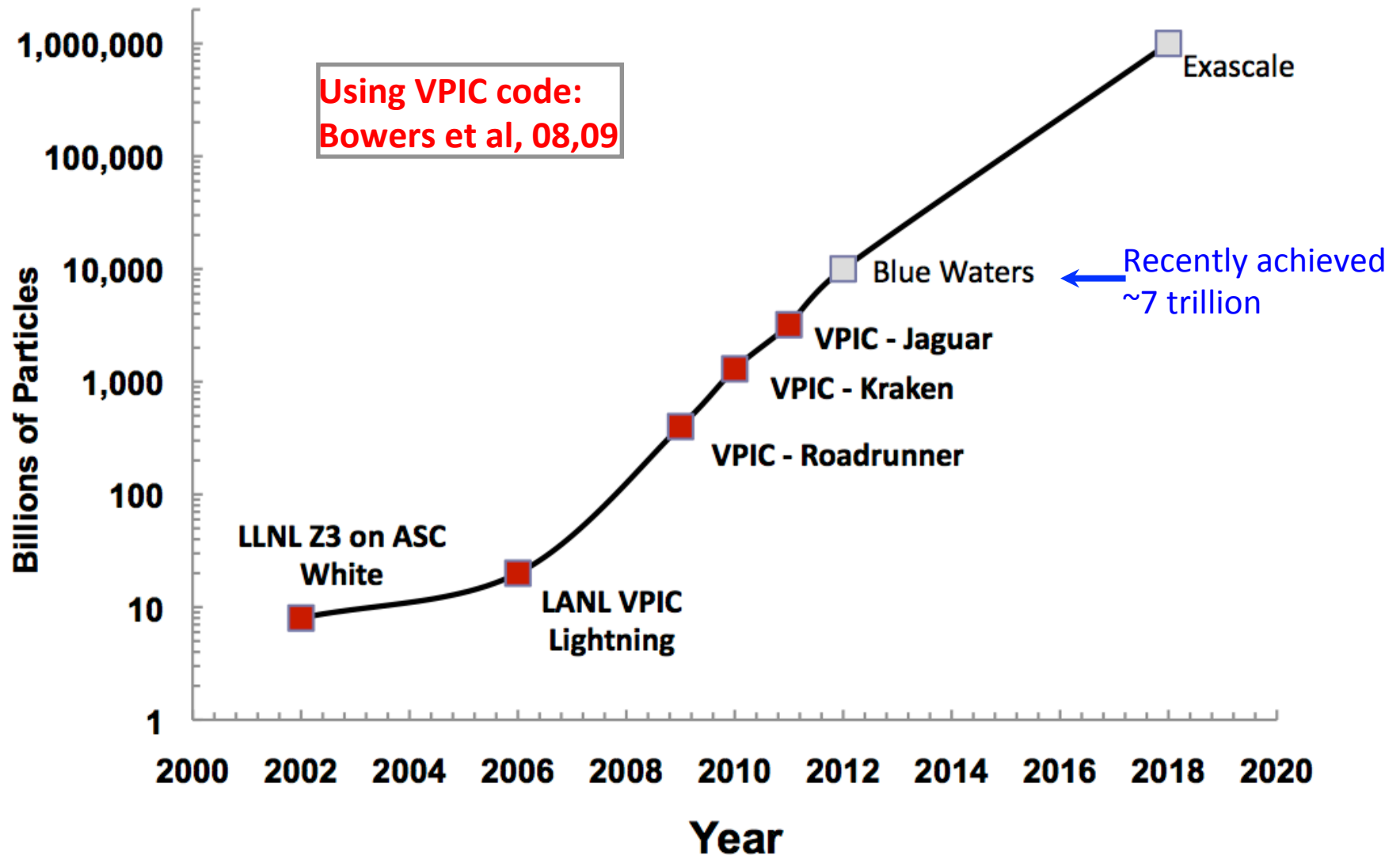
- Capability to study processes occurring at ion and electron scales (but with artificial mass-ratio), including current layers and dissipation regions with scale separation between ions and electrons,
- Capability to include new equations of state for the anisotropic and tensor electron and ion pressure, with significant implications for energy, magnetic flux, and particle transport during space weather events,
- Capability to handle multiple ion species (such as hydrogen *and* oxygen), thus enabling the coupled treatment of composition, wave and instability dynamics in the magnetosphere, and its implications for the onset of substorms and storms,
- Efficient and flexible computer simulation codes that use state-of-the-art algorithms and scale to up to tens of thousands of processors on modern computational architectures,
- Validation and verification plan to model geospace during storms and substorms that can be tested with spacecraft observations,
- Deliverable to NASA CCMC for community access.

Suite of Codes and V&V

- Next Generation OpenGGCM (Germaschewski and Raeder, Leads)
- Gkeyll: Testbed for testing equation of state closures in multi-fluid formulation (Hakim, Lead)
- Global Hybrid Code H3D (Karimabadi, Lead)
- NASA-GSFC Global Hall MHD Code with GPU accelerators, including multiple ion species (Dorelli and Gloer, Leads)
- Fully Kinetic Codes VPIC (Daughton, Lead) and PSC (Germaschewski, Lead)
- Verification and validation with observations (Chen, Lead).

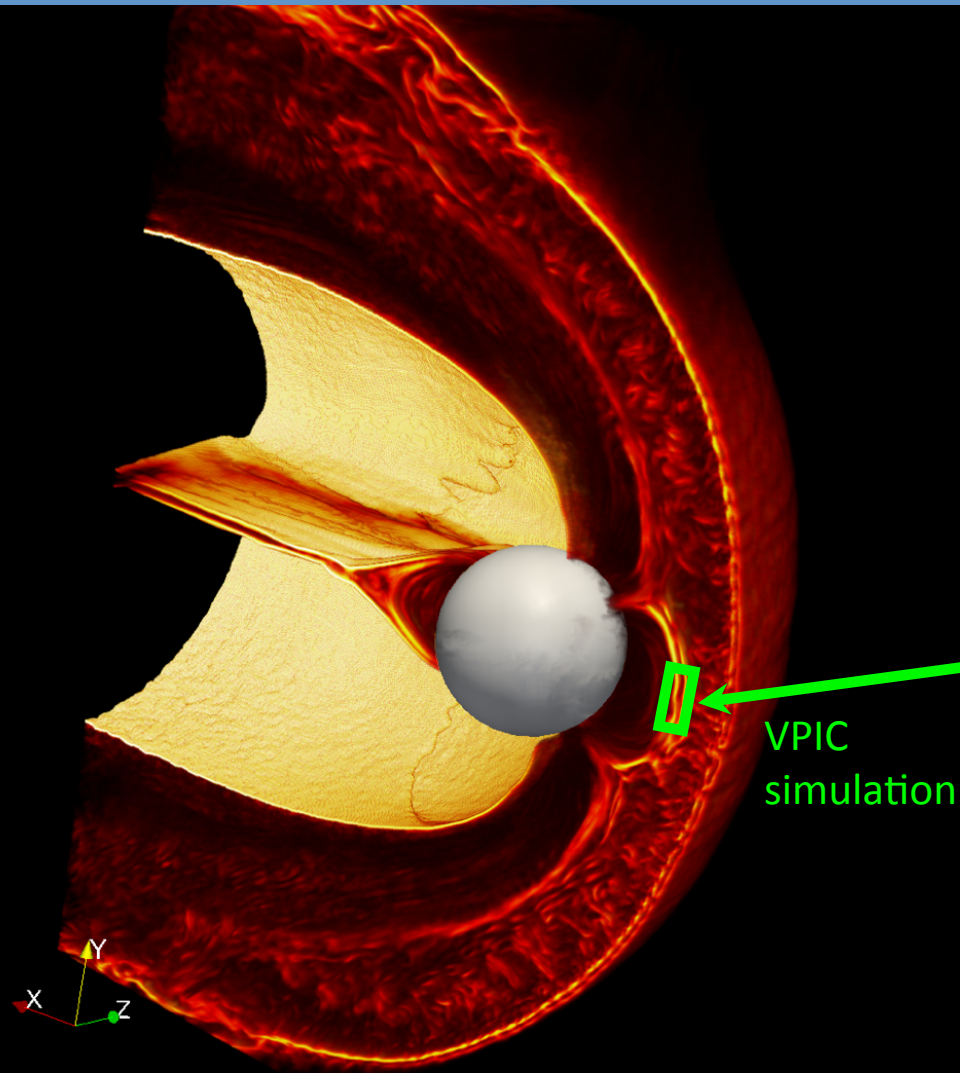
A couple of our codes have won DOE INCITE grants.

VPIC performance



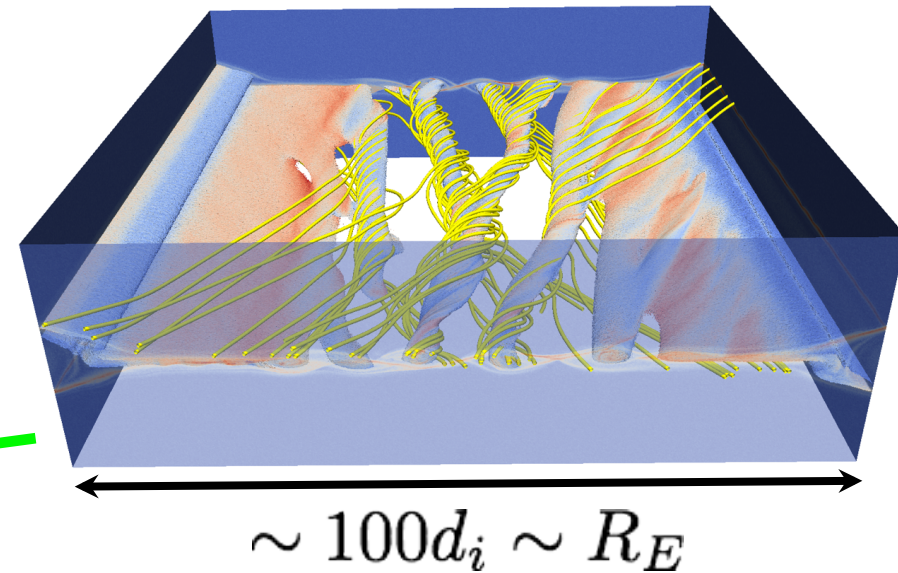
What simulations are feasible at the petascale? (Karimabadi presentation)

Hybrid $\sim 10^{10}$ cells $\sim 10^{12}$ ions



Fully Kinetic

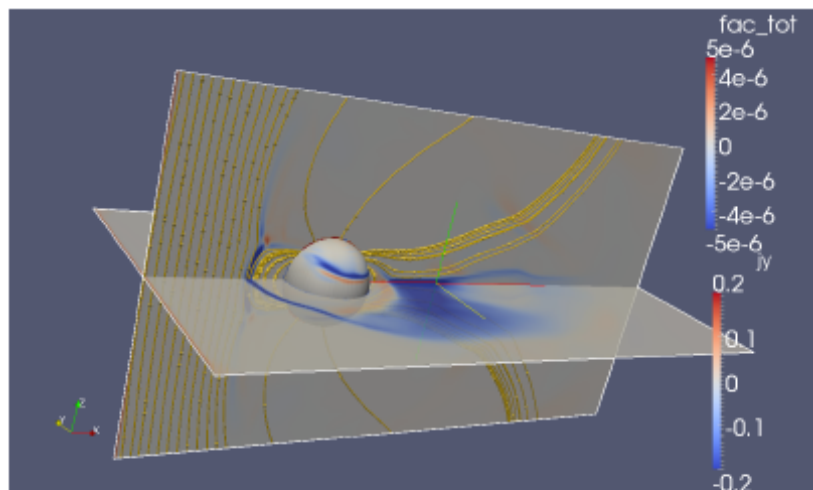
$\sim 10^{10}$ cells $\sim 10^{12}$ particles



$3D \rightarrow m_i/m_e = 100 - 400$

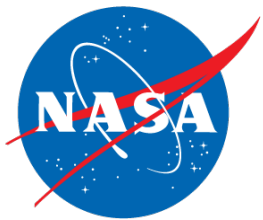
$2D \rightarrow m_i/m_e = 400 - 1836$

Next-generation OpenGGCM

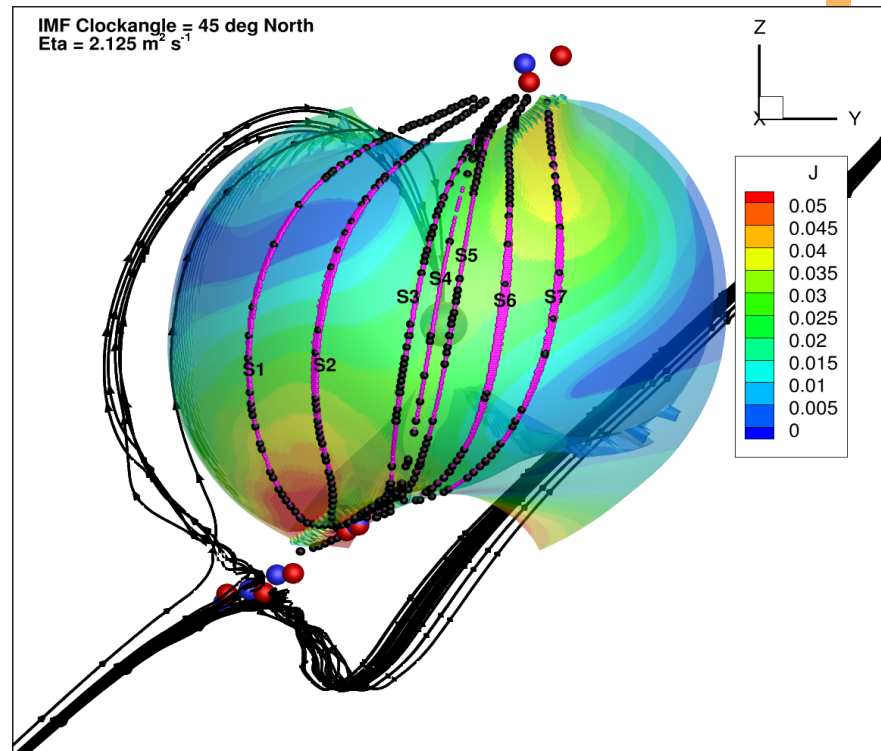
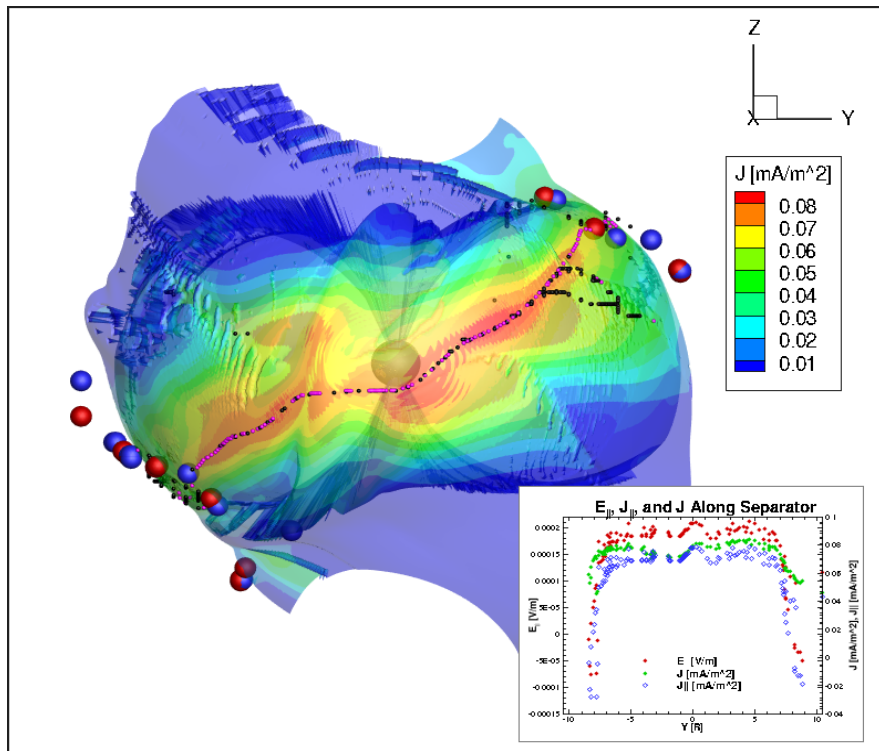
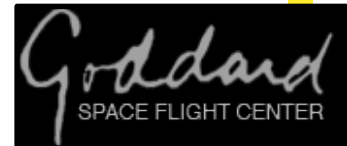


- modular architecture (based on LIBMRC)
- options for fluid plasma models (MHD, XMHD, multi-fluid, pressure tensor closures)
- adaptive mesh refinement
- implicit time integration
- Coupled to CTIM, RCM, CRCM, ...

New components available as open source, whole model to be delivered to CCMC.



Computing the reconnection rate in Earth's magnetosphere



Works in more complicated situations (FTEs, multiple separators....)

- The current density is maximized on (and parallel to) the separator, in contrast to the Cassak-Shay picture of asymmetric reconnection.
- Most of the contribution to the integrated parallel electric field occurs in the subsolar region (even when current density peaks in the cusps).
- To compute the global rate of open flux generation, one must locate the "dominant separator(s)" (just as in 2D).





Earth is hard...we start with Ganymede



Ganymede



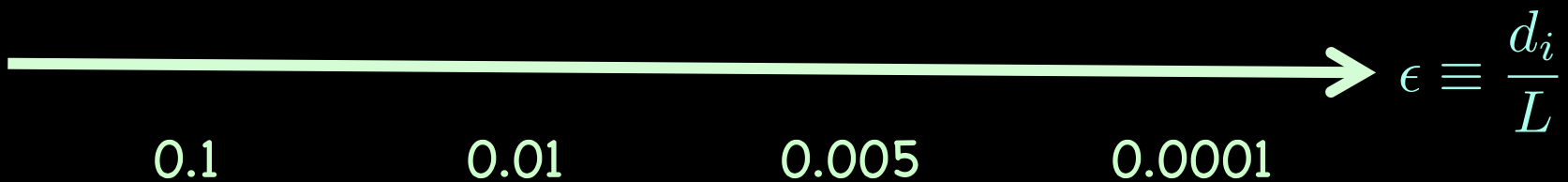
Mercury



Earth



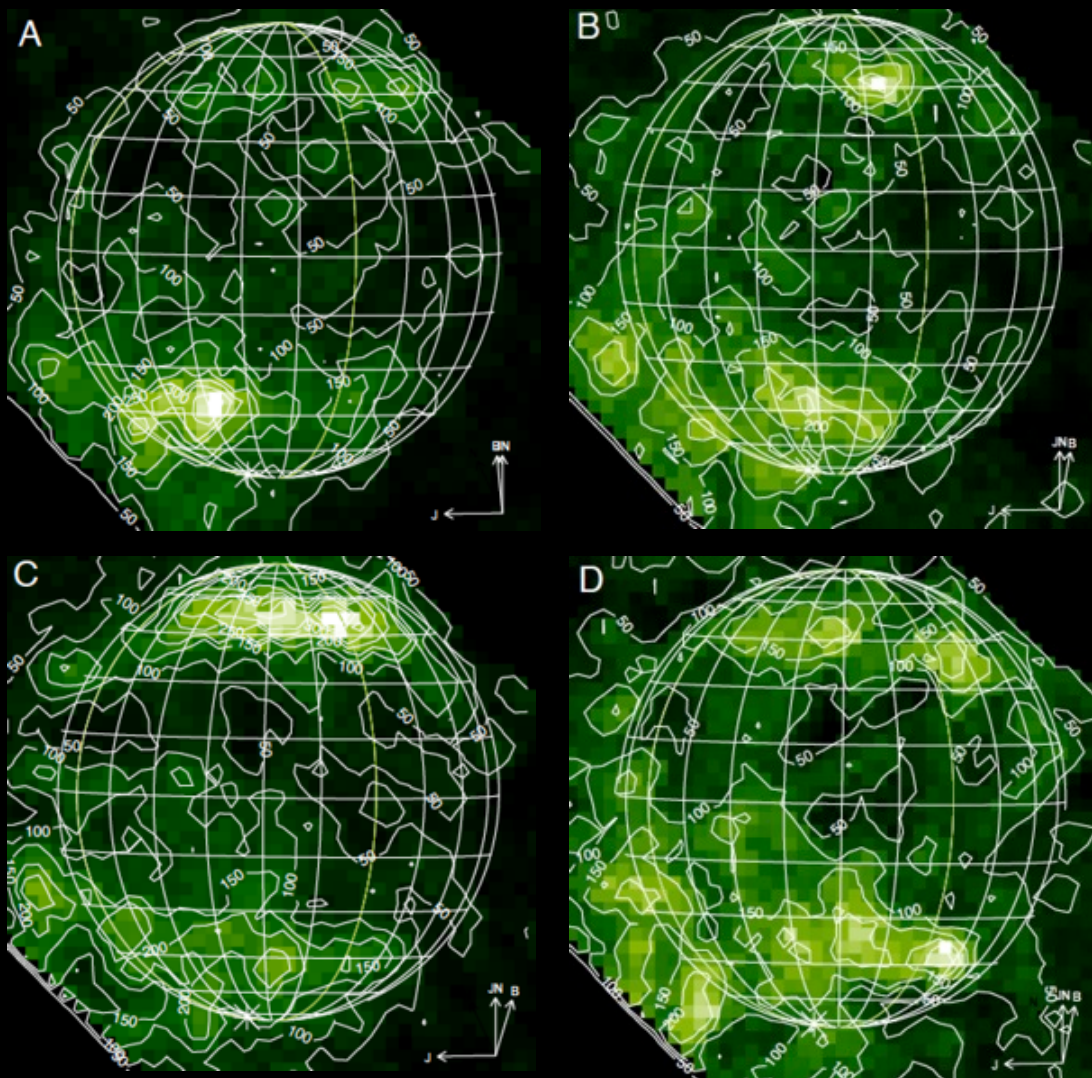
Jupiter



We expect the Hall effect to shape the global structure and dynamics of Ganymede's magnetosphere (Germaschewski, next presentation)



Magnetic Reconnection and Ganymede's Aurora



Feldman *et al.*, *Ap. J.*, 2000.

- First observed by Hall *et al.*, *Ap. J.*, 1998.
- Consistent with electron impact dissociation of O_2
- Spatial and temporal variability is difficult to explain if we assume homogeneous O_2 atmosphere and electron fluxes
- Is there an electron acceleration process analogous to that at Earth?

High level issues for the predictive modeling of magnetic reconnection in global models

1. Build-up and onset

Where & when does reconnection occur ?

2. Time scales

Local vs global reconnection rates

Feedback between micro & macro scales

When does reconnection turn off ?

How much flux is reconnected ?

3. Where does the energy go?

Fast flows vs ion & electron heating

Highly energetic non-thermal tails

Need reduced models that capture some of these effects in global codes, while avoiding unnecessary details in predictive global codes.

Multi-fluid models of plasmas are obtained by taking moments of Vlasov equation

Describe *each species* of the plasma as moments of the Vlasov equation

$$\frac{\partial f_s}{\partial t} + v_j \frac{\partial f_s}{\partial x_j} + \frac{q_s}{m_s} (E_j + \epsilon_{kmj} v_k B_m) \frac{\partial f_s}{\partial v_j} = 0$$

Truncate moment system by a closure scheme.

Five-moment model consists of equation for number density, momentum and scalar pressure.

Ten-moment model consists of replacing scalar pressure with a self-consistent equation for all six component of the pressure tensor, with a closure for the heat-flux tensor.

Electromagnetic fields are evolved with the full Maxwell equations, retaining displacement currents. I.e. Ohm's law is *not* used to compute electric field.

These models treat all species of plasma on same footing

Unlike asymptotic models like Hall-MHD or resistive MHD, moment models include electron inertia, do not assume quasi-neutrality, include displacement currents, and, in ten-moment model, include self-consistent equations for pressure tensor. Additional species and “streams” for a species, can be added with minimum modifications.

Hall currents, separate pressures equations for electron and ions, diamagnetic (and other) drifts, and FLR effects from pressure tensor are included automatically, and **not via an Ohms Law or auxiliary equations.**

Coupling between species is only via Lorentz and current sources. Hence, each species and the EM field can be evolved independently, potentially with different algorithms and time-steps.

Five- and ten-moment models differ on how pressure and heat-flux are handled

Equations for number density and momentum for each species,

$$\partial_t n_s + \nabla \cdot (n_s \mathbf{u}_s) = 0$$

$$\partial_t \mathbf{u}_s + \mathbf{u}_s \cdot \nabla \mathbf{u}_s + \frac{1}{mn} \nabla \cdot \mathbf{P}_s = \frac{q}{m} (\mathbf{E} + \mathbf{u}_s \times \mathbf{B})$$

are coupled to Maxwell equations

$$\partial_t \mathbf{B} + \nabla \times \mathbf{E} = 0$$

$$\partial_t \mathbf{E} - c^2 \nabla \times \mathbf{B} = -\frac{1}{\epsilon_0} \sum_s q_s n_s \mathbf{u}_s.$$

Five-moment model treats pressure as *scalar*, $\mathbf{P}_s = p_s \mathbf{I}$, with either an isothermal (T_s constant) or adiabatic EOS

$$\partial_t p_s + \mathbf{u}_s \cdot \nabla p_s = -\gamma p_s \nabla \cdot \mathbf{u}_s$$

In low-frequency limit five-moment model reduces to Hall-MHD

Reduction to Hall-MHD

In the low-frequency limit (no plasma or EM waves) the five-moment model reduces to a Hall-MHD model that *retains* electron inertia *and* separate pressure equations for the electrons and ions. Formally, one can take the limit as $c \rightarrow 0$, $|n_i - n_e| \rightarrow 0$ and $m_e/m_i \rightarrow 0$ to obtain the Hall-MHD approximation.

Often Hall-MHD models do not include “ ∇p_e ” terms, and set electron mass to zero⁶. This makes comparisons of five-moment results with such Hall-MHD results difficult.

Quadratic dependence of Whistler wave on wave-number is absent in five-moment model (in which the Whistler transitions to an electron cyclotron wave), and hence may be advantageous when using explicit schemes.

Quadratic dependence of Whistler wave on wave-number is absent in five-moment model

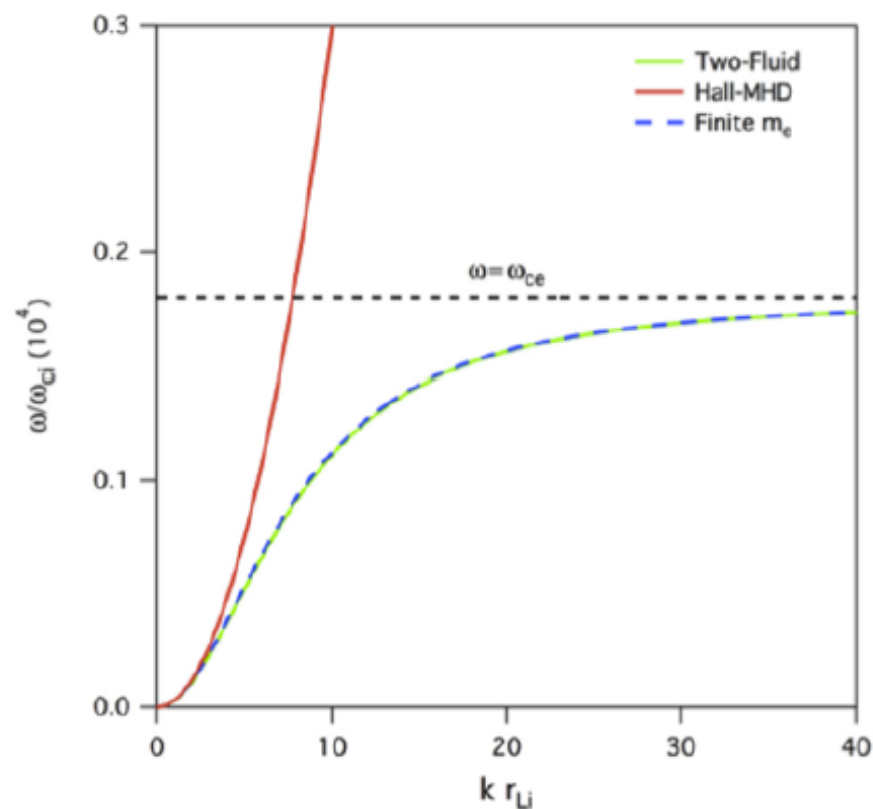


Figure: The whistler dispersion of the five-moment plasma model, compared to Hall-MHD model with and without electron inertia. Finite electron inertia allows the whistler wave to have an asymptote at the electron cyclotron frequency whereas ignoring electron inertia causes it to grow quadratically. This can lead to Δx^2 dependence of time-step for explicit Hall-MHD algorithms, absent in five-moment models.

Five- and ten-moment models differ on how pressure and heat-flux are handled

Ten-moment model retains all six components of the pressure tensor. A self-consistent time-dependent equation is used

$$\partial_t P_{ij} + u_k \partial_k P_{ij} + P_{ij} \partial_k u_k + \partial_k u_{[i} P_{j]k} + \partial_k Q_{ijk} = \frac{q}{m} B_m \epsilon_{km} [i P_{jk}]$$

Square brackets around indices represent symmetrization. For example, $u_{[i} P_{j]k} = u_i P_{jk} + u_j P_{ik}$.

A closure is needed to determine $\partial_k Q_{ijk}$. One could use even higher moments⁵, but some forms of higher moment equations have issues of realizability, i.e. may lead to distribution functions that are negative in some parameter space. Problem of closure does not go away.

Five moment model has $5S + 8$ equations, while ten-moment models have $10S + 8$ equations, where S is number of species.

Our presently implemented closure: Hammett-Perkins (1990)

$$\partial_m Q_{ijm} \approx v_t |k_0| (P_{ij} - p \delta_{ij})$$

Closure can be improved further as we progress in the project

- Superficially, this closure looks like a collisional relaxation. However, note that the closure really is non-local, and involves averaging along field lines (or in a box). Such averaging will be implemented soon.
- At first sight one may think that relaxing to a CGL pressure tensor may be better as it takes into account field line structure. However, this (used alone), and as now μ is conserved, prevents fast reconnection. *Some form of isotropization is needed.*
- The closure can be further modified to get the correct kinetic thresholds for the generalized mirror and firehose instabilities. Essentially, once we detect that the pressure anisotropy crosses the kinetic stability threshold, we relax the pressure to bring it back to marginal stability. Similar “trick” used in GEM studies, accretion disk simulations, and others.
- Fast non-local integration algorithms (A. Dimits, APS 2013) based on Padé approximations for the nonlocal heat flux can be explored.

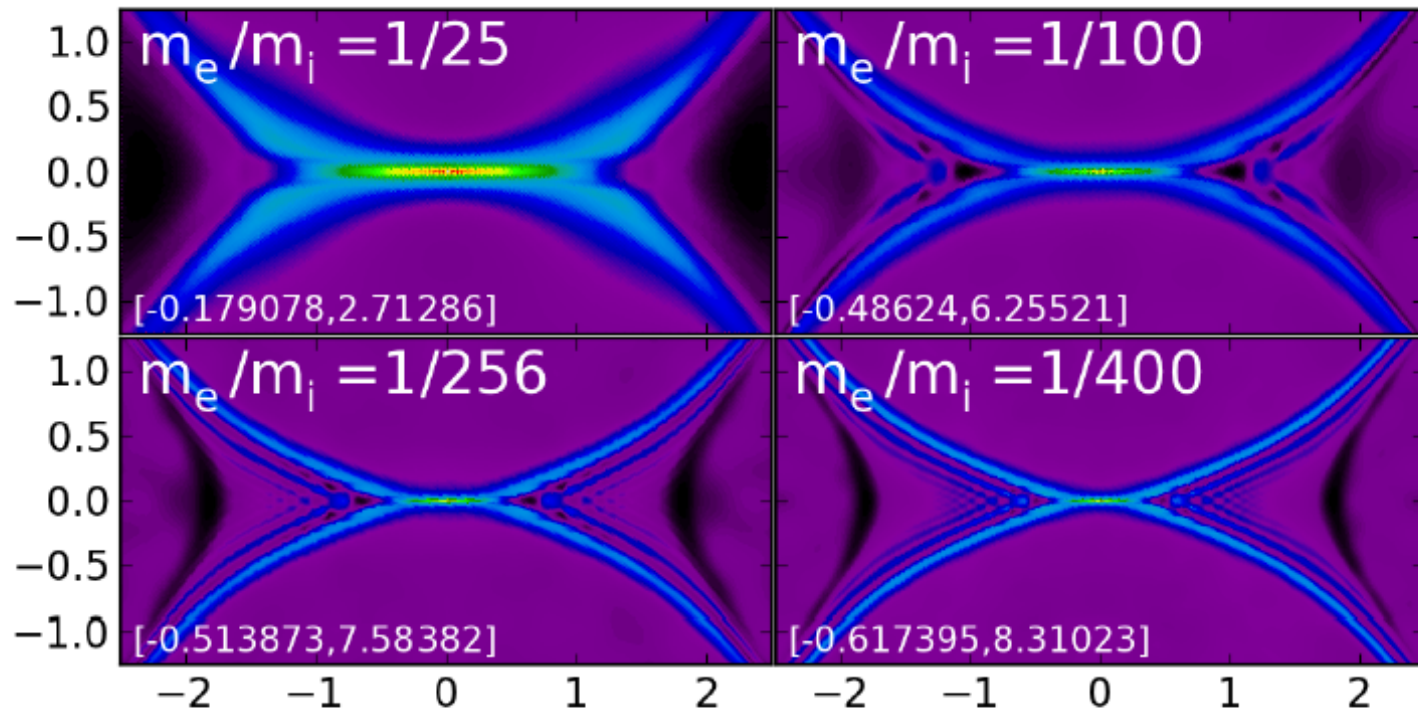
Gkeyll is a C++/Lua package for solution of both (gyro)kinetic as well as multi-fluid equations

Gkeyll was initiated as a project to implement continuum algorithms for the 5D gyrokinetic equations, using discontinuous Galerkin scheme.

- Gkeyll is written in C++ and inspired by framework efforts like Facets, VORPAL (Tech-X Corporation) and WarpX (U. Washington).
- Provides a generic mechanism for implementing solvers, and flexibly composing these to do simulations.
- Programming language Lua, used in widely played games like World of Warcraft, is used as an embedded scripting language to drive simulations.
- MPI is used in parallelization, and HDF5 is used for I/O via txbase library developed at Tech-X.
- A sophisticated meta-build system (developed at Tech-X) is used, and code is version controlled with Mercurial, hosted at www.bitbucket.org.

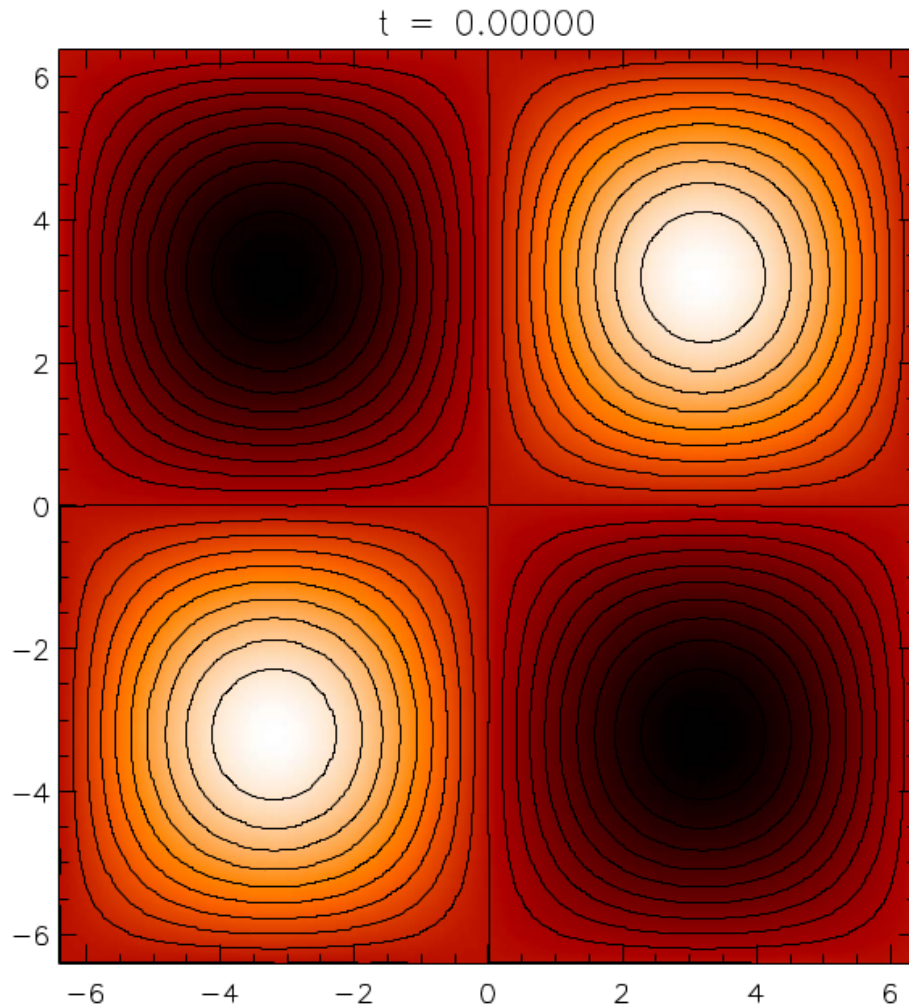
Use of Lua means there is no top-level “main” in the C++ code. Gkeyll is mainly a library, with a simple entry point to load the Lua script, pass it to the interpreter to run. Should allow relatively easy use in other codes.

A website with extensive set of notes and results is maintained. See <http://www.ammar-hakim.org/sj>



Benchmark results of fluid and Maxwell solvers in 1D, 2D and 3D, example applications of five- and ten-moment models, Lua scripts are provided.

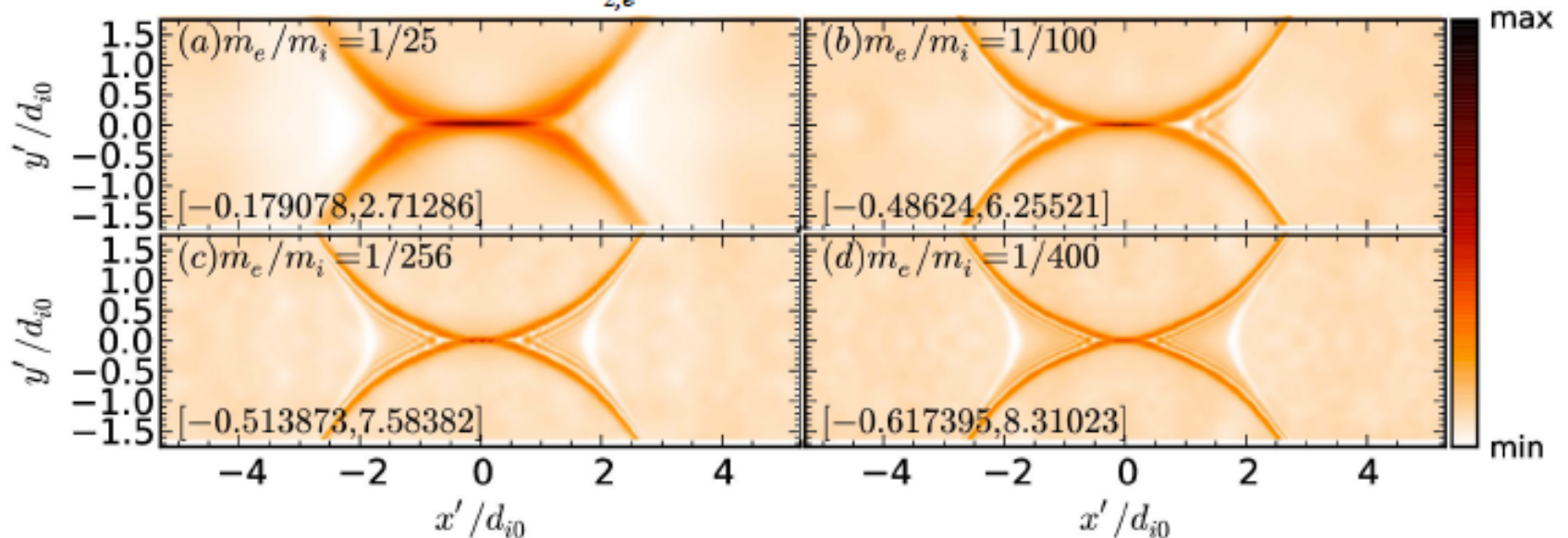
Test problem: Coalescence of flux tubes



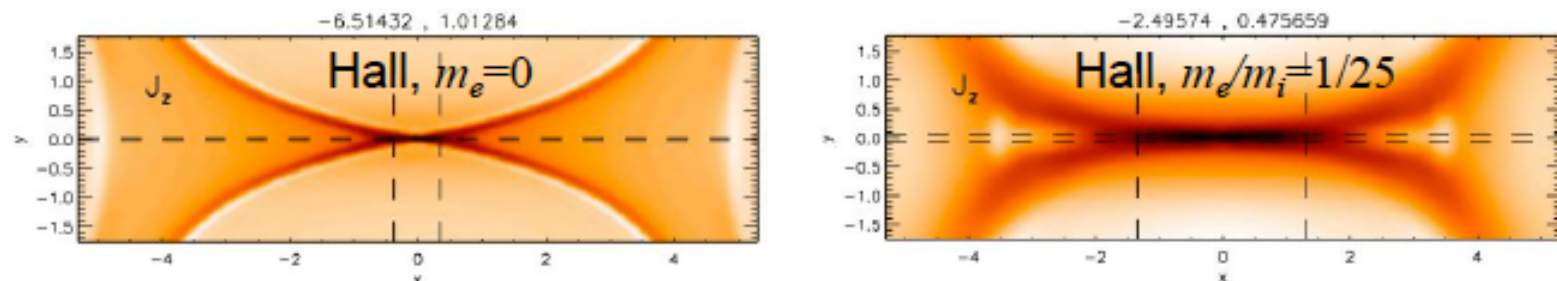
B. P. Sullivan, A. Bhattacharjee
and Y.-M. Huang, Physics of
Plasmas 16, 10211 (2009)

Electron current layer structures in quasi-steady states due to different m_e/m_i

$J_{z,e}$ in Five-Moment run

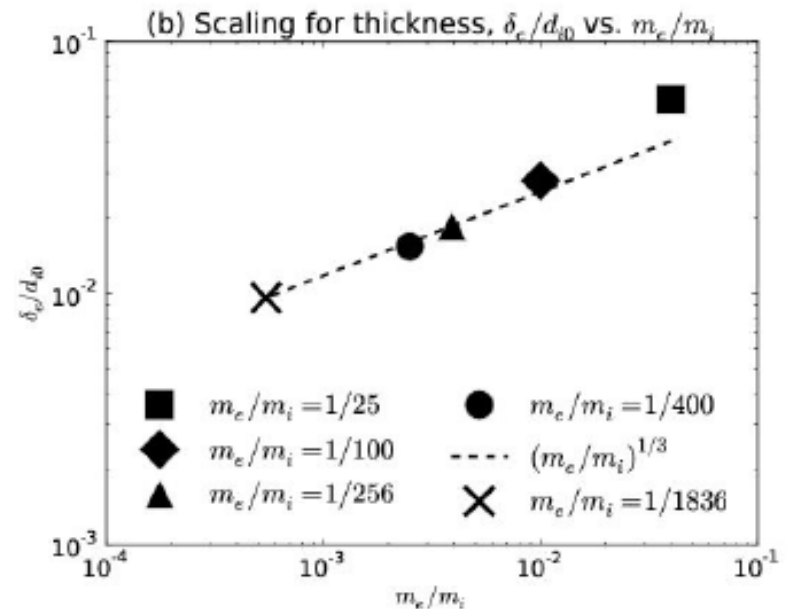
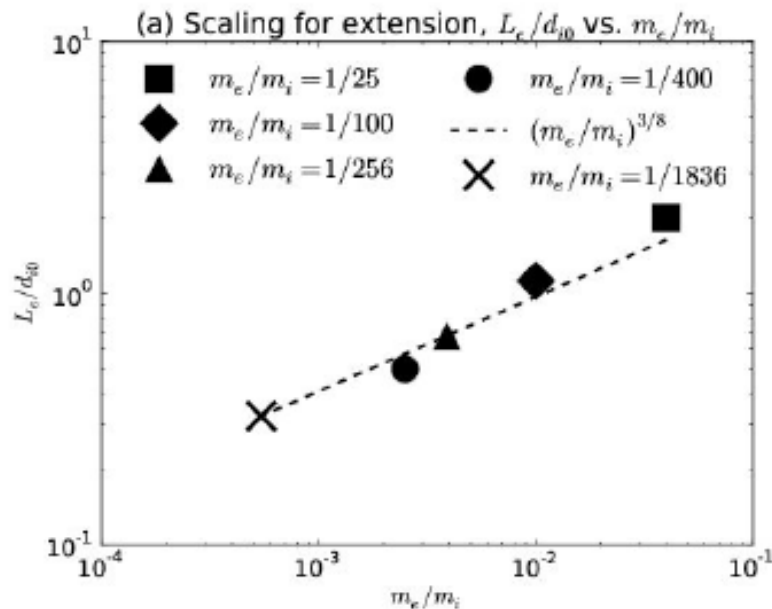


J_z (dominated by $J_{z,e}$) in Hall MHD run^[1]



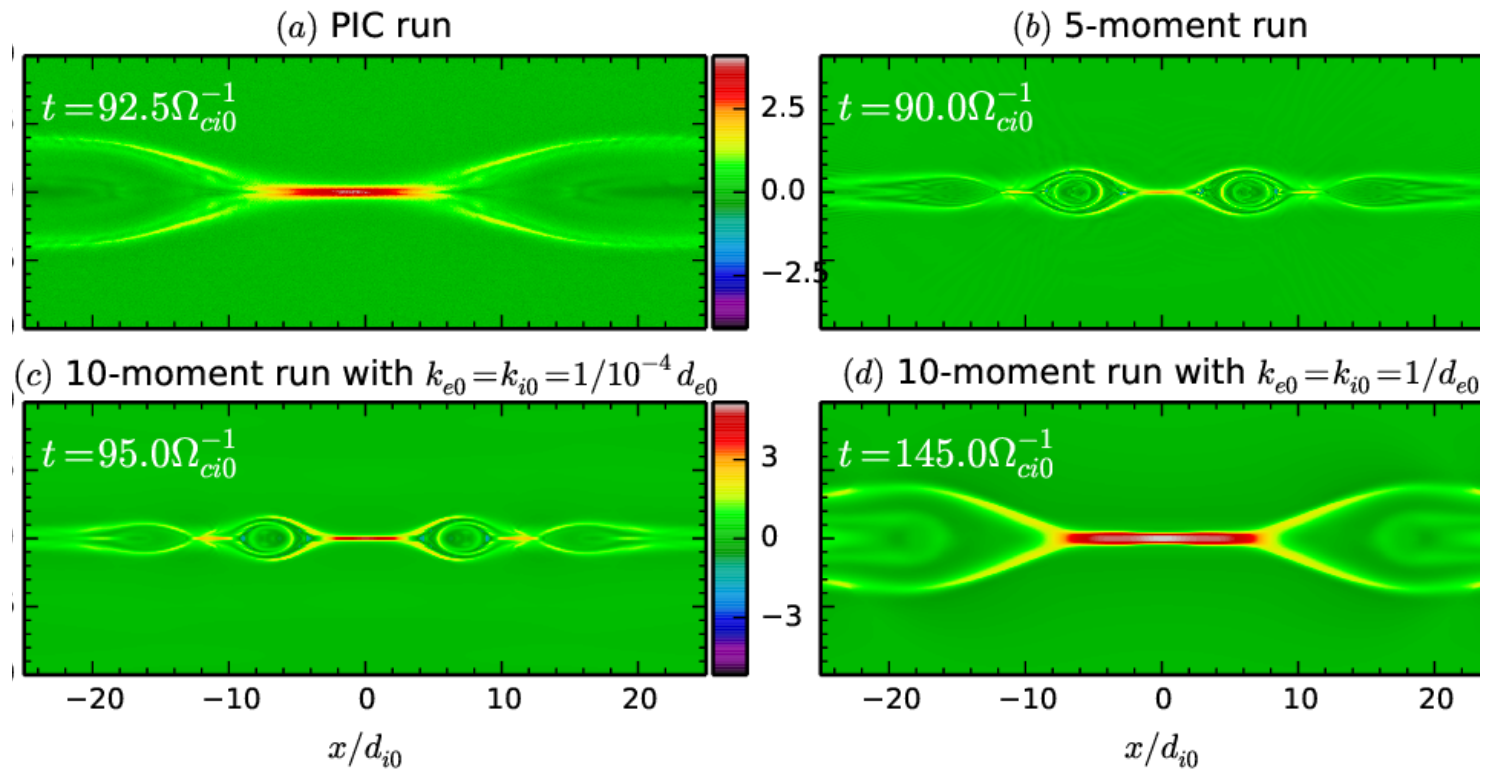
[1] B. P. Sullivan, A. Bhattacharjee, and Y.-M. Huang, Physics of Plasmas 16, 102111 (2009)

Scaling laws for current sheet length L_e and thickness δ_e

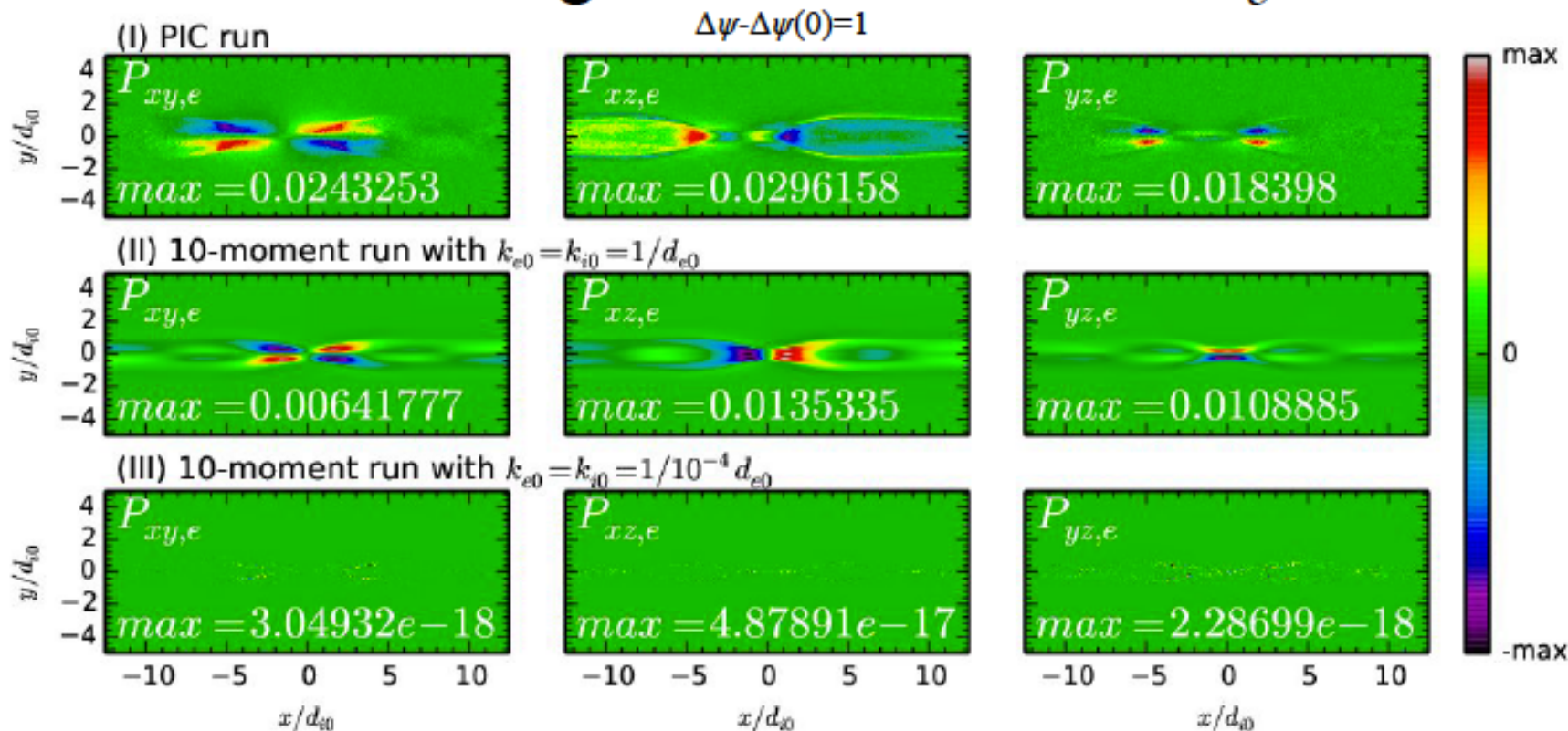


- Estimated scaling law curves are similar to that obtained by *Sullivan et al.*
- Extrapolated value of L_e at realistic mass ratio is about 12 to 17 d_{e0} , or 0.28 to 0.4 d_{i0} , agreeing with that predicted by *Sullivan et al.* ($\sim 15d_{e0}$ or $0.3d_{i0}$)
- Extrapolated value of δ_e is about 0.4 to 0.6 d_{e0} , significantly narrower than that predicted by *Sullivan et al.* ($\sim 1d_{e0}$) but still of same order of magnitude
- Sources of differences?: Measurement errors (limited number of data points, vast range of m_e); Hall runs use a small hyperresistivity and isothermal *EoS*

Out-of-plane electron velocity

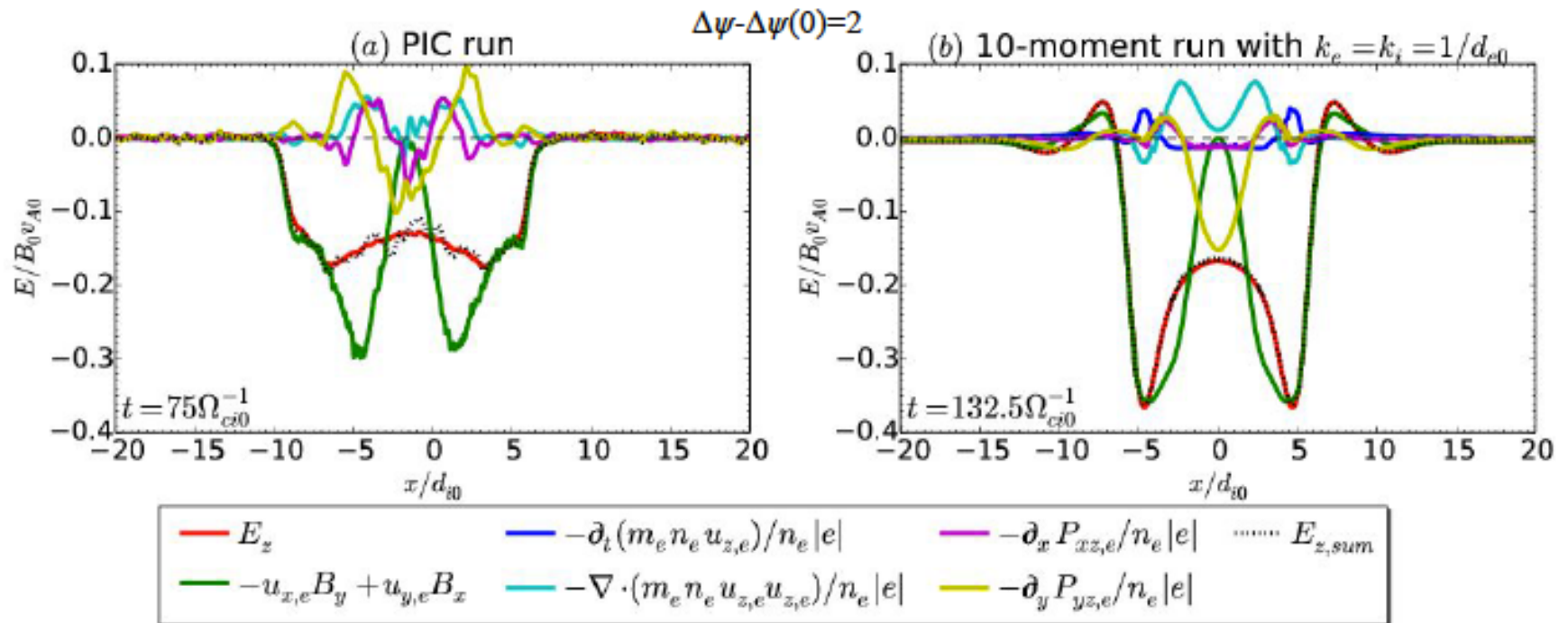


Off-Diagonal elements of P_e



- 10-moment run with $k_e=k_i=1/d_{e0}$ (second row) recovers the qualitative structures, particularly the polarities shown in the PIC run (first row)
- The magnitudes near the X-point in the first two rows are close
- The magnitudes in the further downstream regions are significantly different
- In the 10-moment run with $k_e=k_i=1/10^{-4}d_{e0}$, $P_{xy,e}$, $P_{xz,e}$, and $P_{yz,e}$ vanish!

Decomposition of generalized Ohm's law



- E_z in both runs are mainly supported by $\partial_y P_{yz,e}$ near the X-point, with comparable magnitudes
- Structures of various terms are qualitatively similar
- PIC: $-u_{x,e}B_y + u_{y,e}B_x$ and $\partial_y P_{yz,e}$ cancel in the shoulder regions \Rightarrow flat E_z
- 10-moment run with $k_e = k_i = 1/d_{e0}$: Locations of peaks of the two terms do not overlap, thus little cancellation $\Rightarrow E_z$ overshoots in the side shoulder regions
- Differences might be caused by subtle differences in timing and noises in PIC